



# Sensitivity to water deficit of the second stage of fruit growth in late mandarin trees

Pablo Berríos<sup>1</sup> · Abdelmalek Temnani<sup>1</sup> · Susana Zapata<sup>1</sup> · Manuel Forcén-Muñoz<sup>1</sup> · José Antonio Franco<sup>1</sup> · Alejandro Pérez-Pastor<sup>1</sup>

Received: 23 November 2021 / Accepted: 20 April 2022 / Published online: 14 May 2022  
© The Author(s) 2022

## Abstract

In citrus fruits, phases I and II of fruit growth are sensitive to water deficit, and for this reason, deficit irrigation (DI) has been usually restricted to the final ripening phase. However, the optimal timing and intensity of stress during sensitive phases have not been clearly defined. The main objective was to determine the sensitivity of the second stage of fruit growth to water deficit in adult mandarin trees, and to explore the suitability of different soil and plant water status indicators, including the leaf-scale spectrum, according to the water stress level. Four irrigation treatments were tested: a control (CTL) irrigated at ~80% of  $ET_c$  during the entire crop cycle, and three irrigation suppression treatments, in which no water was applied during the end of phase I and the beginning of phase II ( $DI_1$ ), the second half of phase II ( $DI_2$ ), and phase III of fruit growth ( $DI_3$ ), respectively. Phase II of fruit growth can be considered as a non-critical phenological period until the fruit reaches approximately 60% of its final size, with the application of a water deficit using an irrigation threshold of midday stem water potential of  $-1.8$  MPa, and a cumulative water stress integral close to 28 MPa day. The novel visible infrared ratio index (VIRI) showed a high sensitivity for trees subjected to moderate and severe water stress and can be complementarily used to estimate on a larger temporal and spatial scale the plant water status. Wavelengths in the short-wave infrared (SWIR) region allowed differentiation between non-stressed, moderately, and severely water-stressed trees, and can be considered as an initial basis for determining the water status of mandarin trees at various stress intensities by remote sensing.

## Introduction

Citrus fruit production in Spain covers an area of almost 300,000 ha, and mandarin trees are one of the most important crops, accounting for 35% of the national citrus production. Similarly, in the Region of Murcia, in Southeastern Spain, 5789 ha are cultivated, with an annual production of 120,948 tons. In Spain, the agricultural sector requires 18,409  $hm^3$  of water per year, and the production of fruit crops is the most demanding (Ministerio de Agricultura Pesca y Alimentación del Gobierno de España 2020). It is estimated that currently—due to the effect of climate change—2.4 billion people live in water-scarce basins, and projections indicate that this deficit will increase in a large part of the planet, due to the high sensitivity of water scarcity to the pattern of

climate change (de Nicola et al. 2015; Gosling and Arnell 2016). Therefore, to reduce pressure on water resources and to maintain economic and environmental sustainability, irrigation water use efficiency (iWUE) must be increased. In this sense, deficit irrigation (DI) refers to irrigation below crop requirements during periods in which the crops are not sensitive to water deficit, which allows a significant increase in iWUE (Chalmers et al. 1981; Pérez-Pastor et al. 2009; Conesa et al. 2015; Temnani et al. 2020). However, its success depends on irrigation scheduling according to plant water status, which can be monitored directly or indirectly through several indicators (Jones 2004).

In citrus trees, several studies have evaluated the sensitivity of fruit growth stages to water deficit, but without clearly defining the optimal time and stress intensity. In clementine trees subjected to severe water stress during the three phases of fruit growth, Ginestar and Castel (1996) found that anthesis and fruit set were the most sensitive. Similarly, in sweet orange cv. Lane late trees, irrigation suppression during phase I promoted higher fruit abscission and slower fruit growth (Pérez-Pérez et al. 2008). When severe water deficit

✉ Alejandro Pérez-Pastor  
alex.perez-pastor@upct.es

<sup>1</sup> Departamento de Ingeniería Agronómica, Universidad Politécnica de Cartagena (UPCT), Paseo Alfonso XIII, 48, CP 30203 Cartagena, Murcia, Spain

was applied to clementine trees in phases I and II separately, yield was reduced by 58%, and when water deficit was sustained in both phases, yield was reduced by around 80% (Ginestar and Castel 1996; Pérez-Pérez et al. 2008; Romero et al. 2006). Thus, DI was carried out mainly during fruit ripening period, when the fruit had almost reached its final size and when climatic demand decreased, as it would not affect yield. However, fruit quality can be altered by the increase in peel thickness, total soluble solids, and titratable acidity (Ginestar and Castel 1996; Romero et al. 2006). In this context, the intensity and duration of the water deficit must be clearly identified, as well as the fruit growth phase or even specific moments within them, especially considering that phase II is the longest and occurs during a period of high evaporative demand.

Several indicators of plant or soil water status exist for irrigation scheduling in woody crops, and in this context, stem water potential has been widely validated, due to its high sensitivity and because it is a plant measurement that is directly related to environmental conditions and soil water availability (Shackel et al. 1997; Naor 2000; Marsal et al. 2002; Ortuño et al. 2009; Moriana et al. 2012). However, it is a measurement of low spatial scale and short temporal scale, due to the limited time to measure, and requires trained technicians, which limits its practicality. For this reason, stem water potential should be used as a reference for other indicators (Naor 2000). In this sense, advances in technology such as remote sensing, using unmanned aerial vehicles equipped with broadband multispectral or thermal sensors, allows the remote characterization of a crop's agronomic properties, on a larger spatial scale and longer temporal scale. Furthermore, crop characterization can be improved, when instead of using multispectral data, its spectral signature is obtained, allowing the detection of which narrow bands or regions of the spectrum are more sensitive to the desired characteristic, in our case, the response to different water stress levels in adult mandarin trees.

The objectives of the present research were (i) to determine the sensitivity of mandarin fruit growth stages to water deficit and its effect on agronomic and physiological responses in a context of severe water scarcity, and (ii) to explore new plant water indicators to estimate the stem water potential and to determine the suitability of different indicators of soil and plant water status, including the leaf-scale spectrum, according to the water stress level.

## Materials and methods

### Study site and experimental design

The trial was carried out during the 2019/20 and 2020/21 seasons in a commercial orchard located in Sucina, Murcia

(37°57'30.75"N, 0°56'16.12"W) with adult mandarin trees cv. Clemenvilla (*Citrus reticulata* Blanco) grafted onto cv. Cleopatra (*Citrus × reshni* Hort. ex Tan.). The orchard was established in the year 2000 on a 6 × 4 m planting frame and irrigated using a drip irrigation system with one drip line per row, and four drippers with an irrigation rate of 4 L h<sup>-1</sup> per tree. The fertilization, weeding, pest, and disease control programs were carried out according to commercial management protocols. Fertilizers were applied in liquid solutions via fertigation without varying the amount between treatments. Macronutrients were applied in solutions of N-P<sub>2</sub>O<sub>5</sub>-K<sub>2</sub>O: 0-20-8 and 5-12-0 plus micronutrients chelated with EDTA. The fertilizer units applied during each season corresponded to 198.5 kg N ha<sup>-1</sup>, 72.7 kg P<sub>2</sub>O<sub>5</sub> ha<sup>-1</sup>, and 169.3 kg K<sub>2</sub>O ha<sup>-1</sup>.

The climate in Murcia is dry Mediterranean type, belonging to the Köppen “Bsh” classification, with mild winters, and dry and very hot summers, with an average annual temperature close to 22.5 °C, low rainfall of less than 300 mm, and a reference evapotranspiration of 1435 mm (AEMET 2021; SIAM 2019). The soil is a Calcic Regosol (IUSS Working Group WRB 2015), with a silt loam texture class (7% sand, 70% silt, and 23% clay), a slightly alkaline pH of 7.56, bulk density of 1.20 Mg m<sup>-3</sup>, and a cation exchange capacity of 14.5 cmol kg<sup>-1</sup>.

A randomized experimental design was established with five adjacent trees as an experimental unit and separated by three trees as a border. Four irrigation treatments with three replicates each were tested: a control (CTL) irrigated at ~80% of ET<sub>c</sub> during the entire crop cycle, and three irrigation suppression treatments, where no water was applied during the end of phase I and the beginning of phase II (deficit irrigation, DI<sub>1</sub>), the first half of phase II (DI<sub>2</sub>), and phase III of fruit growth (DI<sub>3</sub>). In the suppression treatments, irrigation was restored once trees reached severe water stress, corresponding to a solar midday stem water potential (Ψ<sub>s</sub>) of ~ -1.8 MPa in mandarin trees cv. Fortune (Conesa et al. 2014), or a seasonal accumulated water stress integral of ~60 MPa day. When irrigation suppression was not applied, trees were irrigated based on actual water availability. Crop evapotranspiration (ET<sub>c</sub>) in the study area corresponded to around 6600 m<sup>3</sup> ha<sup>-1</sup> per season, but the irrigation water availability did not satisfy the estimated water requirement, so the crop was subjected to a sustained deficit irrigation that provided ~50% of the ET<sub>c</sub> throughout the cycle. Crop evapotranspiration (ET<sub>c</sub>) was calculated according to FAO each season, and the crop coefficient (K<sub>c</sub>) was corrected for the area shaded by the tree canopy (Allen et al. 1998). The adjusted K<sub>c</sub> values were as follows: winter recession I: 0.2; winter recession II: 0.25; sprouting: 0.35; bloom: 0.45; fruit set: 0.45 and fruit phase I, II and III: 0.6; 0.5 and 0.4, respectively. Figure 1 shows the irrigation suppression periods for each

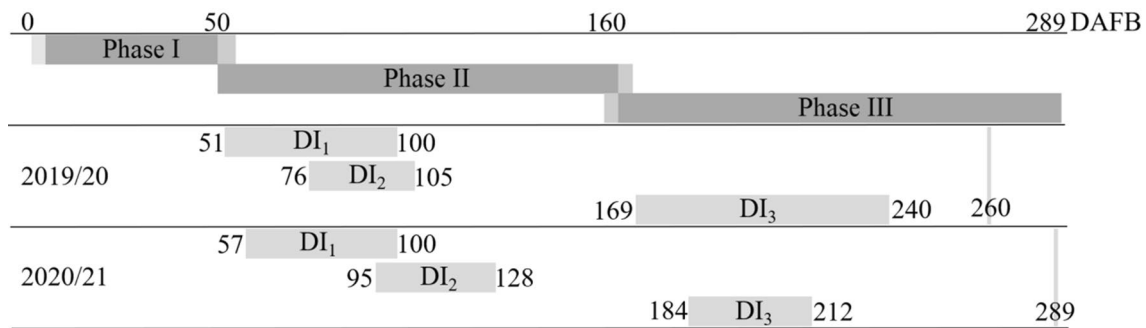


**Fig. 1** Fruit growth phases of adult mandarin trees cv. Clemenvilla (dark grey horizontal bars) and deficit irrigation treatments (grey horizontal bars) applied according to days after full bloom (DAFB)

for both study seasons. Vertical grey lines indicate the harvest day. Full bloom was on the 20th and 24th of April for 2019/2020 and 2020/2021, respectively

treatment and season according to days after full bloom (DAFB).

## Measurements

Reference evapotranspiration ( $ET_0$ ), precipitation, daily mean temperature, and vapor pressure deficit were obtained from the agroclimatic station ‘Cabezo de Plata’ (SIAM 2019).

The weekly evolution of stem water potential at solar midday ( $\Psi_s$ ) was monitored using a Scholander-type pressure chamber model Pump-Up (PMS Instrument Company, USA), on nine shaded adult leaves per treatment, which were located close to the main branches. The leaves were covered with an aluminized bag 1.5 h before measurement. The water stress integral for each irrigation suppression treatment was determined with regard to CTL from Eq. 1 (Myers 1988):

$$S_{\Psi} = \left| \sum_{i=0}^{i=i} (\Psi_{i,i+1} - \Psi_{CTL})n \right|, \quad (1)$$

where,  $S_{\Psi}$  = water stress integral (MPa day);  $\Psi_{i,i+1}$  = solar midday stem water potential for each time interval  $i$ ;  $\Psi_{CTL}$  = control treatment stem water potential and  $n$  = number of days between two consecutive measurements.

Leaf gas exchange was measured as net photosynthesis (Pn) and leaf stomatal conductance (Lc) measured at solar midday in six sunny adult leaves per treatment with the same frequency as the  $\Psi_s$  measurements, corresponding to the first fully expanded adult leaf of a shoot located in the upper middle third of the canopy, using a portable gas exchange system CIRAS-2 (PP Systems, Hitchin, Hertfordshire, UK). The established  $CO_2$  concentration was  $\approx 400 \mu\text{mol mol}^{-1}$ , and photosynthetic photon flux density was  $1200 \mu\text{mol m}^{-2} \text{s}^{-1}$ . Temperature and relative humidity corresponded to the environment during the measurements.

Volumetric soil water content ( $\theta_v$ ) was measured at a 0.5 m depth with a capacitive sensor model 10HS (METER Group Inc., USA) per repetition, installed at 0.1 m from the dripper in the wetting bulb closest to the tree. Data were acquired every minute and averaged every 15 min.

Trunk diameter fluctuation (TDF) was monitored in three trees per treatment using a linear variable displacement transducer (LVDT) sensor model DF (Solartron Metrology, UK), installed 40 cm above the soil on the main trunk and mounted on aluminium and invar holders. The TDF data were acquired every minute and averaged every 15 min. Weekly maximum trunk diameter and trunk growth rates were calculated.

An unmanned aerial vehicle (UAV) model Matrice 600 Pro (DJI Technology Inc., China) with a multispectral sensor, model RedEdge-MX™ (MicaSense®, USA), was used to determine the vegetative growth such as ground cover (%) at harvest. To determine the ground cover from multispectral images, first the normalized difference vegetation index (NDVI) was calculated to differentiate vegetation from ground, then the Otsu’s unsupervised learning method was applied to separate the image into two classes (Kittler and Illingworth 1985), and finally the vegetation cover area was calculated using open-source software ImageJ (Schneider et al. 2012). Ground cover (%) was calculated in four trees per replicate as the ratio between the area covered by the canopy ( $\text{m}^2$ ) and the planting frame ( $24 \text{ m}^2$ ) multiplied by 100 (Raj et al. 2020).

To determine the leaf-scale spectrum, a portable spectroradiometer model FieldSpec® 3, with a contact reflectance probe and its own light source (ASD Inc., USA), was used to collect reflectance data from 20 leaves per replicate. The spectral range was 350–2500 nm with a resolution of 1.4 nm in the 350–1000 nm range, and 2 nm in the 1000–2500 nm range. The measurements were taken at solar midday and on sun-exposed mature leaves from the upper middle third of each tree, and each measurement corresponded to the average of ten

scans. This data was taken in 2020/2021 just before irrigation was restored in the suppression treatments, corresponding to 14, 18, and 30 weeks after full bloom for DI<sub>1</sub>, DI<sub>2</sub>, and DI<sub>3</sub>, respectively. The spectroradiometer provides the reflectance automatically every 1 nm, but due to the wavelength being close to each other, they are generally highly correlated, and, to remove redundant information, the spectrum data were filtered to obtain reflectance every 10 nm (Thenkabail et al. 2011).

To explore new indices from narrow hyperspectral bands and to optimize the fit in the estimation of stem water potential by linear regression, the  $\lambda$ -by- $\lambda$  method was used to determine the combination of bands that allows the best fit as  $R^2$  with the response variable (Darvishzadeh et al. 2008; Yu et al. 2015; Thenkabail et al. 2011).

To determine the response of plant water status on leaf reflectance, the evaluated trees were separated into three groups according to the intensity of water deficit, which was based on  $\Psi_s$  (González-Altozano and Castel 1999; Conesa et al. 2014; Ballester et al. 2014): (i) no water stress,  $\Psi_s > -0.9$  MPa; (ii) moderate stress,  $-0.9 \geq \Psi_s \geq -1.3$  MPa, and (iii) severe stress,  $-1.3 > \Psi_s \geq -1.8$  MPa.

A sensitivity analysis for the different plant water stress indicators was carried out using two methodologies:  $S = SI \cdot CV^{-1}$  (Goldhamer and Fereres 2001) and  $S^* = (SI - 1) \cdot CV^{-1}$  (de la Rosa et al. 2014). Signal intensity (SI) was calculated as the ratio between the deficit and control treatment average values, and sensitivity as the ratio between SI and the average coefficient of variation (CV, noise) of the original variables during the deficit irrigation period.

To determine the yield and productivity, four trees per replicate were harvested during both seasons. Likewise, yield was determined as kilograms of fruit with commercial grade per tree. Productivity was expressed as kg per m<sup>2</sup> of canopy zenith area. Fruit load was expressed as the total number of fruits per tree, and fruit fresh weight as the ratio between kg per tree and the number of fruits harvested. Irrigation water use efficiency (iWUE) was determined as kg of fruit per m<sup>3</sup> applied.

The data obtained were subjected to an ANOVA, and when differences between treatments were detected, the means were separated with Duncan's test ( $p < 0.05$ ) with the InfoStat software (Di Renzo et al. 2019). The  $\lambda$ -by- $\lambda$  method and the exploration of the linear regression models were performed with the "Statistical functions (scipy.stats)" module in Python 3.9.7 (Python Core Team, 2015).

## Results

### Water applied and soil water content

During the experimental period, the accumulated reference evapotranspiration (ET<sub>0</sub>) was around 1380 mm, reaching the

highest values of 6.92 and 6.78 mm day<sup>-1</sup> in 2019/20 and 2020/21, respectively, during the summer, mainly 13 weeks after full bloom. Also, in both seasons, average temperature and vapor pressure deficit values were 19 °C and 1.05 kPa, respectively, with maximum around 30 °C and 2.50 kPa (Fig. 2A, B).

During the first season, rainfall amounted to 620.7 mm and was mainly concentrated at full bloom and when the fruit diameter was 42 mm. On the other hand, in 2020/21, rainfall was half that of previous season and was concentrated before flowering (Fig. 2A, B).

During the experimental period, the control treatments received an average of 5248 m<sup>3</sup> ha<sup>-1</sup>, which represented 40% of ET<sub>0</sub>. The DI treatments saved 44.1, 45.5, and 47.6% compared to the CTL in the first season, and 39.2, 42.5 and 42.5% in the second season, for DI<sub>1</sub>, DI<sub>2</sub> and DI<sub>3</sub>, respectively (Fig. 2C, D). The deficit irrigation treatments, which corresponded to actual water availability in the study area, supplied 2970 m<sup>3</sup> ha<sup>-1</sup> per year on average, equivalent to around 45% of ET<sub>c</sub>.

The soil volumetric water content ( $\theta_v$ ) in the control treatment ranged between 34.6 and 38.3% in the first season, and between 35 and 40%, in the second, depending on the amount of rainfall. During the deficit irrigation periods,  $\theta_v$  reached the lowest values of 28% at the end of the season. For all the DI treatments when irrigation was restored,  $\theta_v$  recovered to control values in 2 weeks, except for DI<sub>3</sub> in the second season, which took almost 4 weeks to recover (Fig. 3A, B).

### Plant water status

The average midday stem water potential ( $\Psi_s$ ) of the control treatment was around  $-0.84$  MPa, being similar between the two seasons. The maximum and minimum values were reached during the fruit set (April,  $\approx -0.5$  MPa) and third fruit growth stage (October,  $\approx -1.2$  MPa), respectively, depending on the climatic conditions (Figs. 2, 3). When the DI treatments were applied,  $\Psi_s$  was significantly lower than the CTL. During the 2019/20 season, the minimum values were  $-1.64$  and  $-2.02$  MPa for DI<sub>1</sub> and DI<sub>2</sub>, respectively, coinciding with the maximum differences with respect to control (0.98 MPa), and accumulating a water stress integral ( $S_\Psi$ ) of around 28 MPa day. The DI<sub>3</sub> treatment presented a minimum of  $-1.67$  MPa, and the differences with respect to CTL were lower but significant. In the second season, the minimum values were around  $-1.7$  MPa, being similar among the deficit treatments, coinciding with the maximum differences with respect to the control treatment of 1.0 MPa (Fig. 3).

Net photosynthesis (Pn) and leaf stomatal conductance (Lc) evolution were similar between seasons. The Pn values ranged between 2 and 16  $\mu\text{mol CO}_2 \text{ m}^{-2} \text{ s}^{-1}$ , showing a

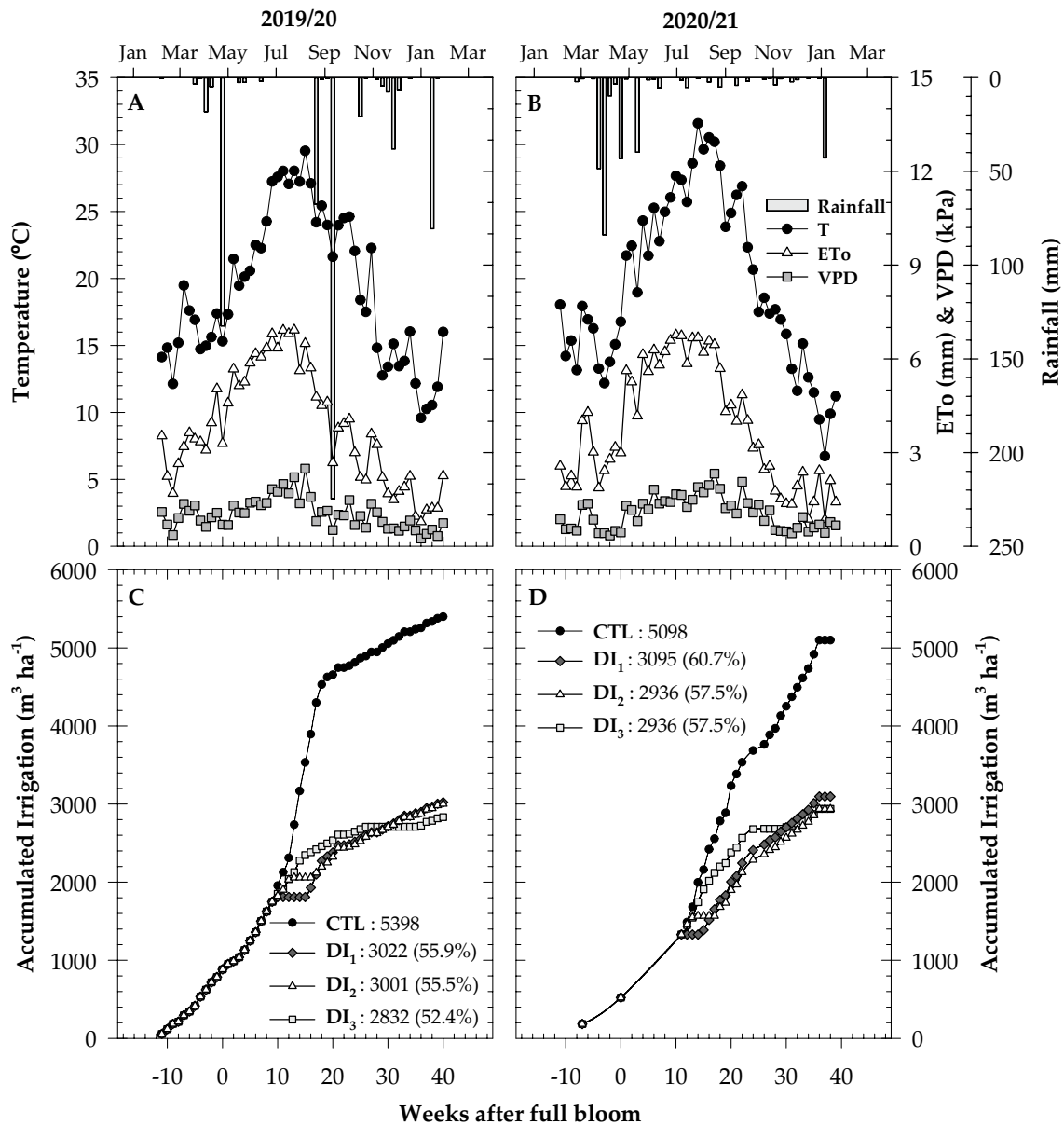


**Fig. 2** Seasonal evolution (2019/20 and 2020/21) of weekly average temperature, reference crop evapotranspiration (ETo), vapor pressure deficit (VPD) and weekly accumulated rainfall for each season (A, B). Weekly accumulated irrigation and total irrigation water volume

for each treatment (C, D). Numbers in brackets indicate the irrigation water used percentage in relation to the CTL treatment. Full bloom was on the 20th and 24th of April for 2019/2020 and 2020/2021, respectively

significant increase until the fruit reached 70% of its final size (35 mm). Lc showed a similar trend to Pn, especially during the second season, with values oscillating between 70 and 150 mmol m<sup>2</sup> s<sup>-1</sup>. Pn values were considerably reduced in the DI treatments, with less significant differences from the control than those observed in Ψs. Furthermore, the DI effect on Lc was not very clear, especially in the DI<sub>2</sub> treatment in the second season (Fig. 4C, D).

### Trunk and fruit growth

The maximum trunk growth rate in the control treatment trees occurred during fruit phase II, being between 200 and 400 μm per week, until it slowed significantly before the fruits reached their final size in phase III. Trunk diameter decreased significantly due to the DI treatments

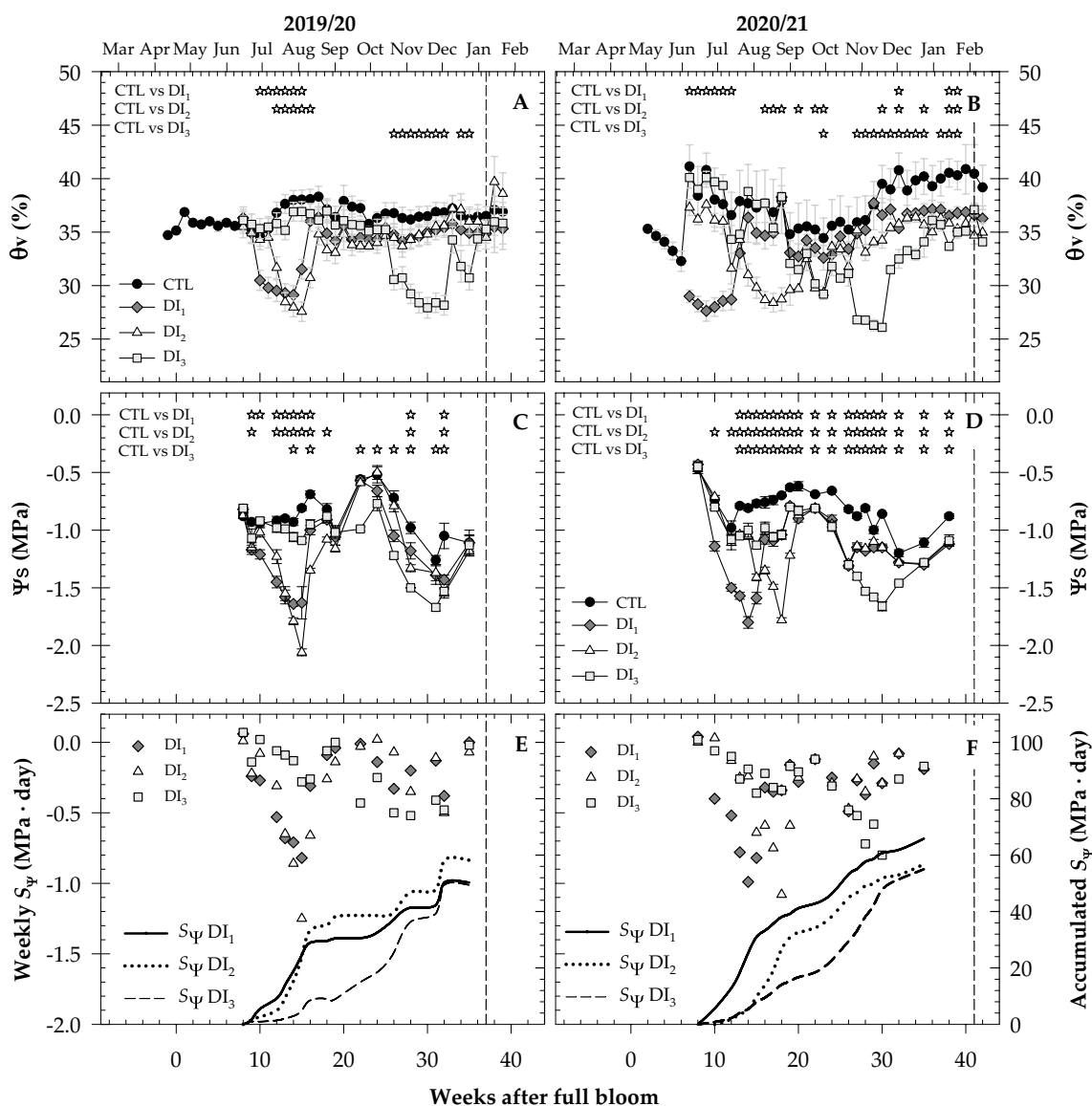


**Fig. 3** Seasonal evolution (2019/2020 and 2020/2021) of volumetric soil water content ( $\theta_v$ ) at 0.5 m depth (A, B); daily stem water potential ( $\Psi_s$ ) at solar midday (C, D) and weekly (marks) and accumulated water stress integral (lines) ( $S_\Psi$ ) (E, F). Vertical dashed line indicates harvest week for each season. Means  $\pm$  standard error,  $n=3$ . White

stars indicate significant differences between each irrigation suppression treatment (DI<sub>1</sub>, DI<sub>2</sub> and DI<sub>3</sub>) to control (CTL) according to Duncan's multiple range test ( $p < 0.05$ ). Full bloom was on the 20th and 24th of April for 2019/2020 and 2020/21, respectively

during phase II (DI<sub>1</sub> and DI<sub>2</sub> treatments), with a reduction of about 50%, as compared to the control. In contrast, DI<sub>3</sub> reduced trunk growth by 25% during phase III. The DI treatments slightly affected fruit diameter, to a greater extent in DI<sub>2</sub> and DI<sub>3</sub> during the first season. When irrigation was restored in the DI treatments, only the fruit diameter recovered to values similar to the control, due to its compensatory growth, and no significant differences between treatments were detected at harvest (Fig. 5A–F).

### Yield components and iWUE

Yield averaged 109.3 and 34.7 kg tree<sup>-1</sup> in the first and second season, respectively, with no significant differences between irrigation treatments. The values for fruit load and productive efficiency were in accordance with the yield from each season. The average fruit weight was also altered due to this, but in addition, the effect of the water deficit significantly reduced the fruit weight in the DI<sub>2</sub> and DI<sub>3</sub> treatments with respect to the control, only during the

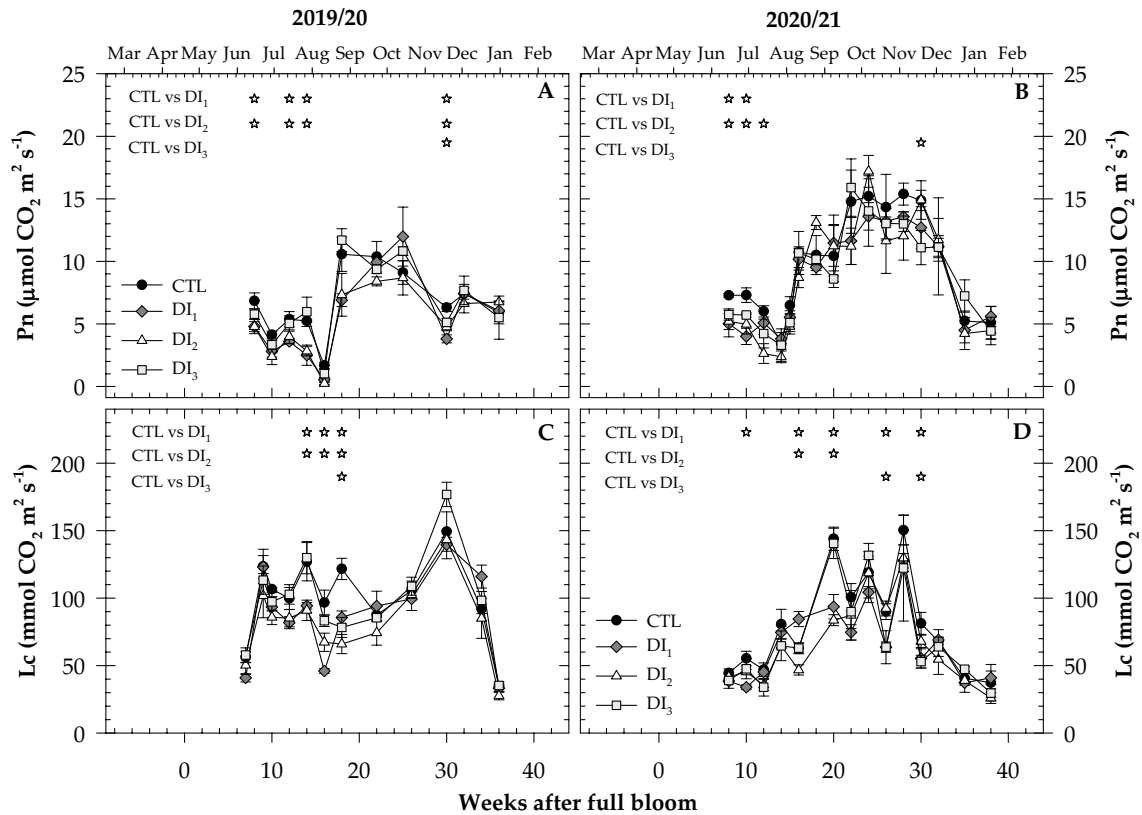


**Fig. 4** Seasonal evolution (2019/2020 and 2020/2021) of leaf gas exchange: net photosynthesis (Pn) (**A**, **B**) and leaf stomatal conductance (Lc) (**C**, **D**). Means  $\pm$  standard error,  $n=3$ . White stars indicate significant differences between each irrigation suppression treatment

(DI<sub>1</sub>, DI<sub>2</sub> and DI<sub>3</sub>) to control (CTL) according to Duncan's multiple range test ( $p < 0.05$ ). Full bloom was on the 20th and 24th of April for 2019/2020 and 2020/2021, respectively

first season. The DI treatments increased iWUE by 87.4 and 65.5% with respect to the control for 2019/20 and 2020/21, respectively. In the DI<sub>3</sub> treatment, no significant differences were detected in the second year as compared to the control (Table 1).

### Leaf-scale spectrum response to water stress

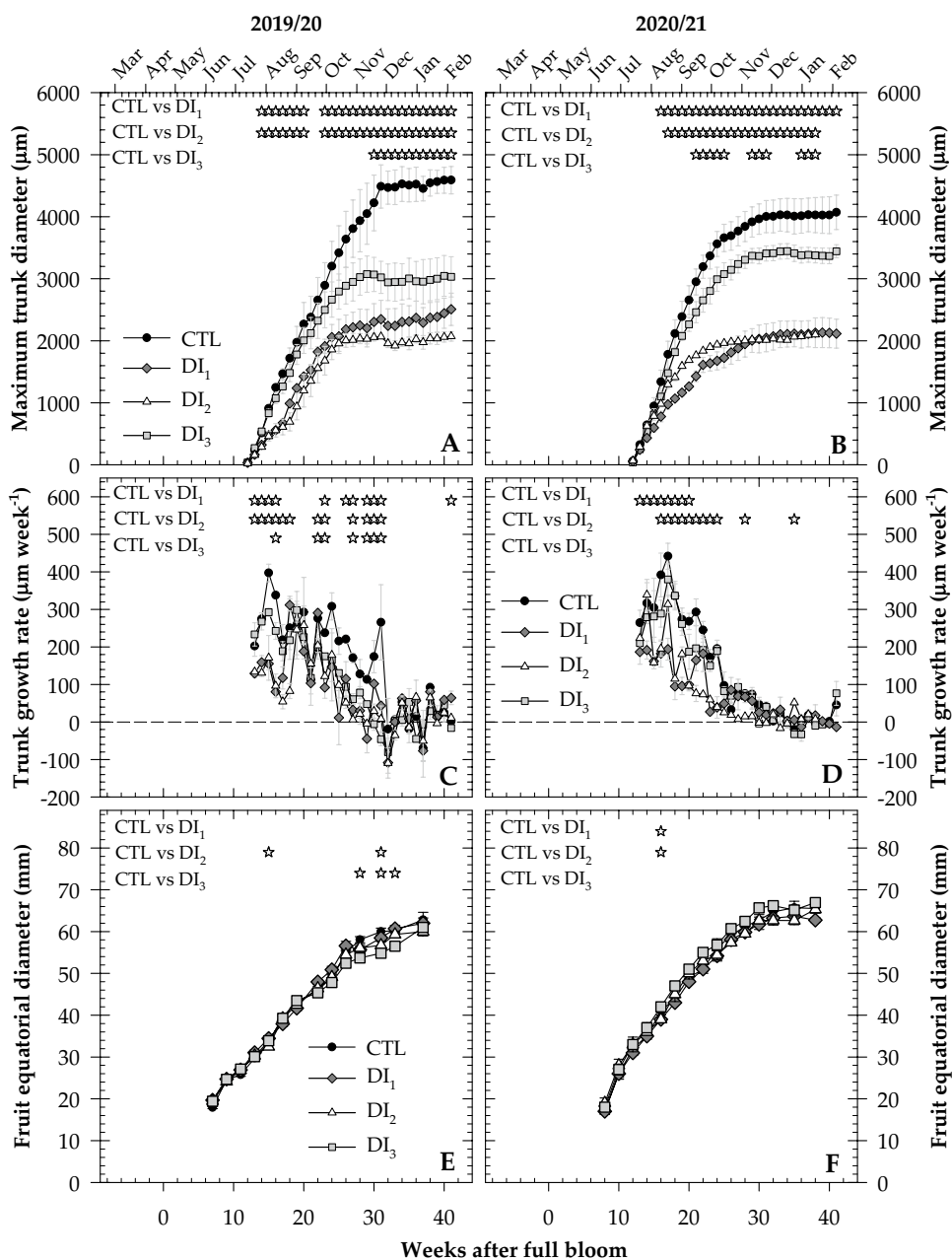
Leaf-scale spectrum was sensitive to severe water stress in a large part of the wavelengths. The leaves showed a higher reflectance and were significantly different from trees without water stress, except for 370–480 (blue), 530–580 (green), 700–720 (red edge), 1880–1980, and greater than 2400 nm from short-wave infrared (SWIR) region. In the case of moderately water-stressed trees, reflectance was significantly higher in trees without water stress in the near-infrared (NIR) region (except for 930–990 nm), and in the range of 1530–1780 nm of the SWIR region. The single hyperspectral narrow band 1000 nm, and the range between 1540 and 1740 nm (SWIR) significantly differentiated the three different water stress intensities (Fig. 6).

### Composition of narrow bands hyperspectral vegetation indices for stem water potential estimation

The  $\lambda$ -by- $\lambda$  methodology allowed two-band combinations and the inclusion of narrow bands as constants to optimize different index structures and determine their fit in predicting stem water potential ( $R^2$ ). Although the linear combinations, including an NDVI-like index, showed a significant fit, the  $R^2$  was relatively low for the prediction. By incorporating the narrow bands detected as constants in the index structure, as they are sensitive to different levels of water stress in the NIR (1000 nm) and SWIR (1640 nm) regions, it was possible to increase the prediction fit to an  $R^2$  of 0.37. In this sense, the new visible infrared ratio index (VIRI), proposed by the combination of the narrow bands described in Eq. 2 (Table 2 and Fig. 6), allowed us to significantly estimate the stem water potential according to Eq. 3 (Table 2):

$$VIRI = (R_{370}/R_{680}) / (R_{1000} \cdot R_{1640}), \quad (2)$$

**Fig. 5** Seasonal evolution (2019/2020 and 2020/2021) of maximum trunk diameter (**A, B**), trunk growth rate (**C, D**) and fruit equatorial diameter (**E, F**). Means  $\pm$  standard error,  $n = 3$ . White stars indicate significant differences between each irrigation suppression treatment ( $DI_1$ ,  $DI_2$  and  $DI_3$ ) to control (CTL) according to Duncan’s multiple range test ( $p < 0.05$ ). Full bloom was on the 20th and 24th of April for 2019/2020 and 2020/2021, respectively



$$\hat{\Psi}_s(\text{MPa}) = -2.97 + 0.5183 \cdot \text{VIRI} (R^2 = 0.37^{***}). \quad (3)$$

$\Psi_s > \theta_v > \text{VIRI} > R_{1640} \approx R_{1740}$ , for both the moderate and severe water-stressed trees (Table 3).

### Indicator sensitivity analysis to moderate and severe water stress

The SI values from the highest to lowest were  $\Psi_s$ , TGR,  $R_{500}$ , and VIRI for severe and moderate water stress levels. Regarding the sensitivity as S, the hyperspectral narrow band reflectance ( $R_{910}$ ,  $R_{970}$  and  $R_{1180}$ ) were in general 1.5 times higher than the  $\Psi_s$ , but when calculating the sensitivity as  $S^*$ , these indicators were non-sensitive. Therefore, the most sensitive indicators under severe water stress were

### Discussion

Phase II of fruit growth can be considered as a non-critical phenological period until the fruit reaches approximately 60% of its final size, for the application of a water deficit using an irrigation threshold of midday stem water potential of  $-1.8$  MPa, and a cumulative water stress integral close to 28 MPa day. The  $DI_1$  strategy allowed increasing the irrigation water use efficiency (iWUE) by an average of



**Table 1** Yield components and irrigation water use efficiency (iWUE)

Season/treatment	Yield kg per tree	Fruit load Fruits per tree	Productivity kg m <sup>-2</sup> canopy	Fruit weight g FW	iWUE kg m <sup>-3</sup>	IWR %
2019–2020						
CTL	107.5 ± 6.2a	1388 ± 100a	12.3 ± 5.5a	77.8 ± 1.6a	8.3 ± 0.5c	–
DI <sub>1</sub>	97.4 ± 7.7a	1342 ± 147a	10.3 ± 0.8a	73.3 ± 2.5ab	13.4 ± 1.1b	44.1
DI <sub>2</sub>	109.3 ± 2.7a	1667 ± 83a	14.8 ± 1.9a	65.8 ± 1.7b	15.2 ± 0.4ab	45.5
DI <sub>3</sub>	123.3 ± 14.0a	1833 ± 279a	13.5 ± 0.7a	68.4 ± 3.4b	18.1 ± 2.1a	47.6
2020–2021						
CTL	35.3 ± 2.1a	280 ± 15a	3.8 ± 0.3a	127.6 ± 7.7a	2.9 ± 0.2c	–
DI <sub>1</sub>	35.8 ± 2.9a	304 ± 39a	3.6 ± 0.3a	119.4 ± 4.4a	4.8 ± 0.5ab	39.3
DI <sub>2</sub>	41.4 ± 7.2a	302 ± 53a	5.4 ± 1.3a	136.5 ± 1.9a	5.9 ± 1.0a	42.5
DI <sub>3</sub>	26.3 ± 2.2a	205 ± 18a	3.1 ± 0.6a	128.2 ± 3.0a	3.7 ± 0.3bc	42.5
Season (S)	***	***	***	***	***	
Treatment (T)	ns	ns	ns	ns	***	
S × T	ns	ns	ns	ns	***	

Means ± standard error,  $n=4$ . Different letters for the same column and season indicate significant differences according to Duncan' test ( $p < 0.05$ )

IWR irrigation water use reduction compared to CTL treatment

\*\*\* $p < 0.05$  and ns non-significant, according to the ANOVA

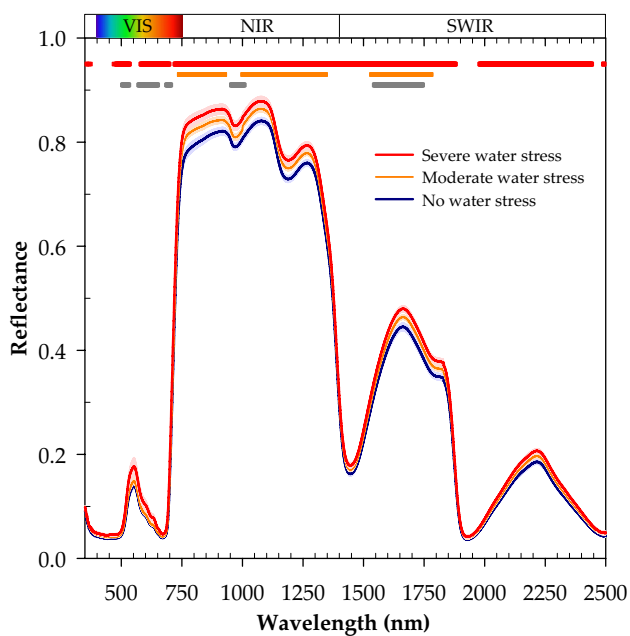


**Fig. 6** Leaf-scale spectrum of adult mandarin trees under severe, moderate and no water stress. Means ± standard error,  $n=9$ . Red, orange, and grey horizontal upper lines indicate significant differences between water stress intensity for each wavelength: severe and non-stress, moderate and non-stress and moderate and severe, respectively; according to the ANOVA ( $p < 0.05$ )

63.4%, without negatively affecting fruit weight. This was also found by Pagán et al. (2022) in late mandarin trees, considering a threshold value of  $-1.9$  MPa, and a seasonal water stress integral of 55 MPa day, on a later cultivar than

the one in our study. For this reason, the application of a water deficit in *Citrus* during the summer would be justified, as stated by González-Altozano and Castel (2000).

This increase in the iWUE may be associated with the compensatory growth of control levels observed in citrus fruits subjected to water deficit, after recovery from irrigation deficit (Cohen and Goell, 1988; Huang et al. 2000; Pagán et al. 2022; Romero et al. 2006), and their capacity to maintain the photosynthetic rate even when water supply was reduced by 50% (Zhihui et al. 1990). Even though the water deficit caused a reduction in trunk growth, the yield was not affected during the following study season. Also, as observed in our study, net photosynthesis was higher mainly during phase II (Fig. 4), coinciding with that reported by Pérez-Pérez et al. (2008), who also indicated that osmotic adjustment and fruit load may determine the magnitude of water use reduction (Pagán et al. 2022). Although the volume of water used between seasons was similar, the iWUE was significantly lower in the second season, given that the final fruit load was almost 80% lower than in 2019/2020, including the trees in the control treatment, so the yield was markedly reduced. This behaviour of alternate bearing is frequent in *Citrus* and in the variety under study (Georgiou 2000). To achieve an increase in the iWUE, it is also necessary to use technology that enables real-time decision making based on various water status indicators obtained from monitoring the soil-plant-atmosphere continuum.

The sensitivity of an indicator to water stress informs us of its viability for use in the delimitation of water deficit in the phenological phases known as non-critical, for the application of regulated deficit irrigation strategies. Thus,

**Table 2** Best narrow bands hyperspectral  $\lambda$ -by- $\lambda$  combinations between 350 and 2500 nm for stem water potential estimation by linear regression ( $Y = \beta_0 + \beta_1 X_1 + \epsilon$ )

Index structure	Wavelength (nm)		$\beta_0$	$\beta_1$	$R^2$	Significance
	$i$	$j$				
$R_i - R_j$	1510	2460	2.54	18.22	0.3079	***
$R_i/R_j$	1020	1030	- 311.1	307.82	0.2783	***
$(R_i - R_j)/(R_i + R_j)$	1020	1030	3.35	620.20	0.2783	***
$(R_i - R_j)^2/R_{1640}$	1520	2460	- 2.03	3123.2	0.3133	***
$(R_i - R_j)^2/R_{1000}$	2390	2450	- 2.29	26,113.3	0.2585	***
$(R_i/R_j)/(R_{1000} \cdot R_{1640})$	370	680	- 2.97	0.5183	0.3706	***

\*\*\*  $p < 0.001$

the signal intensity (SI) was higher when calculated from the indicators observed under severe stress (Goldhamer and Fereres 2004). The indicators showed an SI under moderate water stress conditions ( $-0.9 \geq \Psi_s \geq -1.3$  MPa), with the following order from highest to lowest:  $\Psi_s >$  trunk growth rate (TGR)  $>$   $R_{500}$   $>$  leaf stomatal conductance (Lc)  $>$  Visible Infrared Ratio Index (VIRI)  $>$  volumetric soil water content ( $\theta_v$ ). Similarly, for severe water stress conditions ( $-1.3 > \Psi_s \geq -1.8$  MPa), the SI from the highest to the lowest were: TGR  $>$   $\Psi_s$   $>$   $\theta_v$   $>$   $R_{630}$   $>$   $R_{500}$   $>$  VIRI. Within the hyperspectral narrow bands, the reflectance at 500 nm showed a high SI for moderate and severe stress, and 630 nm only when the stress intensity was severe. Also, in the hyperspectral vegetation indices, the novel VIRI index showed the highest SI in both stress conditions. High SI values may be useful for irrigation scheduling, such as that observed in almond (Goldhamer and Fereres 2004), peach (Conejero et al. 2007), apple (Naor and Cohen 2003), young and old lemon trees (Ortuño et al. 2005, 2006) and grapevine (Ru et al. 2021). However, an optimal indicator, in addition to having a high sensitivity to water deficit, should have a low coefficient of variation (CV) or “noise” (Goldhamer et al. 2000), since the higher the variability, the greater is the uncertainty of the plant water status characterization (Naor and Cohen 2003). In our case, the indicators with a high CV were TGR, leaf reflectance at 500 and 630 nm, and leaf gas exchange components.

The sensitivity ( $S^*$ ) assessment proposed by de la Rosa et al. (2014) allowed for a better discrimination of the effect of low SI, or when there was a CV greater than the increase in SI, which may indicate sensitivity when it did not exist, as the sensitivity of an indicator should be related to the water stress intensity reached by the crop (de la Rosa et al. 2016). In this sense, the indicators with the best performance or sensitivity for trees with moderate and severe water stress corresponded to:  $\Psi_s > \theta_v > \text{VIRI} > R_{1640} \approx R_{1740}$ . Other factors related to the indicators, such as their spatial and temporal scale, implementation costs, data management, and technical

staff requirements for their interpretation, also need to be assessed.

In relation to the leaf-scale spectrum variation as a function of different water stress levels, this response was significantly sensitive in the SWIR region between 1540 and 1740 nm, and particularly in the 1000 nm wavelength in the NIR region. Similarly, Panigrahi et al. (2014) in mandarin trees cv. Kinnow detected a 10–13% higher reflectance in the SWIR region than that achieved in our research, with a minimum  $\Psi_s$  of  $-1.4$  MPa and water stress integrals of 45.8 MPa day, for non-irrigated trees during the early fruit growth period.

## Conclusions

The time and level of water deficit to be applied to adult mandarin trees in semi-arid conditions has been delimited. The irrigation water use efficiency has been increased by 63.4% without affecting crop yield. An irrigation threshold of midday stem water potential of  $-1.8$  MPa and a cumulative water stress integral close to 28 MPa day until the fruits reach 60% of their final size should be considered.

The new hyperspectral indicator, named visible infrared ratio index (VIRI), showed a high sensitivity to water stress, as  $\Psi_s$  and  $\theta_v$ , and can be used as a complement to other indicators of smaller temporal and spatial scales.

Wavelengths in the short-wave infrared (SWIR) region between 1540 and 1740 nm allowed differentiation of non-stressed, moderately, and severely water-stressed trees. Therefore, these results can be considered as an initial basis for determining the water status of mandarin trees at various stress intensities by remote sensing.

## Author contributions

Conceptualization: AP-P and PB; methodology: A P-P, PB and JAF; validation: AP-P and JAF; formal analysis: PB and AT; investigation: AP-P, PB, AT and SZ; writing—original draft preparation: PB and AP-P; writing—review and

**Table 3** Sensitivity analysis of water status indicators of mandarin trees under moderate and severe water stress

Indicators	Moderate water stress − 0.9 ≥ Ψs ≥ −1.3 MPa				Severe water stress − 1.3 > Ψs ≥ −1.8 MPa				
	SI	CV	S	S*	SI	CV	S	S*	
I	Plant water status indicators								
	Stem water potential	1.35	0.07	18.1	4.74	2.21	0.04	48.4	26.5
	Net photosynthesis	1.08	0.55	1.96	0.15	1.02	0.46	2.21	0.06
	Leaf stomatal conductance	1.17	0.16	7.15	1.08	1.00	0.27	3.58	0.01
	Trunk growth rate	1.30	0.84	1.53	0.35	2.30	0.85	2.69	1.52
II	Soil water status indicators								
	Volumetric soil water content	1.11	0.04	25.0	2.53	1.41	0.06	20.63	6.02
III	Hyperspectral narrow bands								
Visible	$R_{500}$	1.25	0.20	6.25	1.25	1.25	0.20	6.25	1.25
	$R_{630}$	1.00	0.16	6.00	0.00	1.33	0.25	5.33	1.33
Near infrared (NIR)	$R_{910}$	1.02	0.03	28.68	0.68	1.05	0.03	30.07	1.40
	$R_{970}$	1.03	0.03	27.68	0.68	1.05	0.04	29.07	1.40
	$R_{1000}$	1.01	0.03	27.67	0.34	1.05	0.04	29.73	1.40
	$R_{1080}$	1.02	0.03	29.35	0.68	1.05	0.03	30.73	1.40
Short-wave infrared (SWIR)	$R_{1180}$	1.03	0.02	38.53	1.03	1.05	0.04	27.07	1.41
	$R_{1260}$	1.03	0.02	40.03	1.03	1.04	0.04	27.37	1.04
	$R_{1440}$	1.06	0.11	9.03	0.53	1.13	0.11	10.13	1.13
	$R_{1540}$	1.03	0.06	16.51	0.51	1.06	0.06	17.56	1.06
	$R_{1640}$	1.05	0.04	24.05	1.05	1.07	0.04	25.10	1.60
	$R_{1740}$	1.05	0.04	21.55	1.05	1.07	0.04	22.61	1.61
	$R_{2200}$	1.05	0.10	10.53	0.53	1.11	0.10	11.61	1.11
Indicators	Moderate water stress − 0.9 ≥ Ψs ≥ − 1.3 MPa				Severe water stress − 1.3 > Ψs ≥ − 1.8 MPa				
	SI	CV	S	S*	SI	CV	S	S*	
IV	Hyperspectral vegetation indices								
Courel et al. (1991)	$GI_n = R_{560}/R_{668}$	1.03	0.09	11.34	0.34	1.09	0.11	9.57	0.82
Gitelson et al. (1996)	$GNDVI_n = (R_{842} - R_{560})/(R_{842} + R_{560})$	1.00	0.07	14.20	0.00	1.04	0.12	8.88	0.37
Courel et al. (1991)	$NDGI_n = (R_{560} - R_{668})/(R_{560} + R_{668})$	1.00	0.16	6.00	0.00	1.02	0.16	6.22	0.11
Rouse et al. (1974)	$NDVI_n = (R_{842} - R_{668})/(R_{842} + R_{668})$	1.01	0.02	45.50	0.50	1.01	0.02	45.50	0.50
Merzlyak et al. (1999)	$PSRI_n = (R_{668} - R_{560})/R_{842}$	1.00	0.25	4.00	0.00	1.17	0.43	2.72	0.39
Gamon and Surfus (1999)	$RGRI_n = R_{668}/R_{560}$	1.03	0.25	4.00	0.13	1.00	0.23	4.29	0.00
Apan et al. (2010)	$DSWI = (R_{803} - R_{549})/(R_{1659} + R_{681})$	1.02	0.07	13.50	0.20	1.06	0.07	15.00	0.89
Hunt and Rock (1989)	$MSI = (R_{1599})/(R_{819})$	1.04	0.03	28.70	1.04	1.06	0.05	22.58	1.33
Apan et al. (2003)	$DSWI_1 = (R_{800})/(R_{1660})$	1.01	0.06	16.27	0.09	1.02	0.05	22.38	0.38
Apan et al. (2003)	$DWSI_2 = (R_{1660})/(R_{550})$	1.00	0.18	5.31	0.02	1.10	0.26	4.21	0.38
Apan et al. (2003)	$DSWI_3 = (R_{550})/(R_{680})$	1.01	0.36	2.79	0.03	1.04	0.36	2.93	0.12
Zarco-Tejada and Ustin (2001)	$SRWI = (R_{860})/(R_{1240})$	1.00	0.02	36.00	0.00	1.01	0.03	36.37	0.34
	$R_{1510} - R_{2460}$	1.00	0.05	20.00	0.00	1.05	0.05	22.05	1.05
	$R_{1020}/R_{1030}$	1.00	0.04	25.00	0.00	1.00	0.05	19.80	0.00
	$(R_{1020} - R_{1030})/(R_{1020} + R_{1030})$	1.06	0.06	16.82	0.91	1.12	0.08	13.21	1.43
	$(R_{1520} - R_{2460})^2/R_{1640}$	1.00	0.04	22.45	0.00	1.09	0.08	13.09	1.09
	$(R_{2390} - R_{2450})^2/R_{1000}$	1.08	0.12	8.80	0.68	1.17	0.14	8.17	1.17
	$VIRI = (R_{370}/R_{680})/(R_{1000} * R_{1640})$	1.11	0.09	11.70	1.15	1.25	0.10	12.87	2.60

Subscript “n” denotes that index was calculated from narrow bands

SI signal intensity, CV coefficient of variation, S sensitivity as SI•CV<sup>−1</sup> and S\* sensitivity as (SI−1)•CV<sup>−1</sup>

editing: AP-P, JAF, PB and AT; visualization: PB, AT and MF-M; field data acquisition: PB, AT, MF-M and SZ; and funding acquisition: AP-P. All authors have read and agreed to the published version of the manuscript.

**Acknowledgements** This study was supported by the European Commission H2020 (Grant 728003, DIVERFARMING Project) and National Research Agency of Spain (PID2019-106226RB-C22).

**Funding** Open Access funding provided thanks to the CRUE-CSIC agreement with Springer Nature.

## Declarations

**Conflict of interest** On behalf of all authors, the corresponding author states that there is no conflict of interest.

**Open Access** This article is licensed under a Creative Commons Attribution 4.0 International License, which permits use, sharing, adaptation, distribution and reproduction in any medium or format, as long as you give appropriate credit to the original author(s) and the source, provide a link to the Creative Commons licence, and indicate if changes were made. The images or other third party material in this article are included in the article's Creative Commons licence, unless indicated otherwise in a credit line to the material. If material is not included in the article's Creative Commons licence and your intended use is not permitted by statutory regulation or exceeds the permitted use, you will need to obtain permission directly from the copyright holder. To view a copy of this licence, visit <http://creativecommons.org/licenses/by/4.0/>.

## References

- AEMET—Agencia Estatal de Meteorología del Gobierno de España (2021) Servicios climáticos: Valores climatológicos normales. <https://www.aemet.es/es/serviciosclimaticos/datosclimatologicos/valoresclimatologicos>. Accessed 11 Oct 2021
- Allen RG, Pereira LS, Raes D, Smith M (1998) Crop evapotranspiration. FAO 56:300
- Apan A, Held A, Phinn S, Markley J (2003) Formulation and assessment of narrow-band vegetation indices from EO-1 hyperion imagery for discriminating sugarcane disease. In: Spatial Sciences Institute Biennial Conference (SSC 2003): Spatial Knowledge Without Boundaries. Spatial Sciences Institute, Canberra, Australia
- Apan A, Held A, Phinn S, Markley J (2010) Detecting sugarcane 'orange rust' disease using EO-1 Hyperion hyperspectral imagery. *Int J Remote Sens* 25:489–498. <https://doi.org/10.1080/01431160310001618031>
- Ballester C, Castel J, El-Mageed TAA et al (2014) Long-term response of 'clementina de nules' citrus trees to summer regulated deficit irrigation. *Agric Water Manag* 138:78–84. <https://doi.org/10.1016/J.AGWAT.2014.03.003>
- Chalmers DJJ, Mitchell PDD, van Heek L (1981) Control of peach tree growth and productivity by regulated water supply, tree density, and summer pruning [trickle irrigation]. *J Am Soc Hortic Sci* 106:307–312
- Cohen A, Goell A (1988) Fruit growth and dry matter accumulation in grapefruit during periods of water withholding and after reirrigation. *Funct Plant Biol* 15:633. <https://doi.org/10.1071/PP9880633>
- Conejero W, Alarcón JJ, García-Orellana Y et al (2007) Daily sap flow and maximum daily trunk shrinkage measurements for diagnosing water stress in early maturing peach trees during the post-harvest period. *Tree Physiol* 27:81–88. <https://doi.org/10.1093/treephys/27.1.81>
- Conesa MR, García-Salinas MD, de la Rosa JM et al (2014) Effects of deficit irrigation applied during fruit growth period of late mandarin trees on harvest quality, cold storage and subsequent shelf-life. *Sci Hortic (amsterdam)* 165:344–351
- Conesa MR, de la Rosa JM, Artés-Hernández F et al (2015) Long-term impact of deficit irrigation on the physical quality of berries in 'crimson seedless' table grapes. *J Sci Food Agric* 95:2510–2520. <https://doi.org/10.1002/jsfa.6983>
- Courel MF, Chamard PC, Guenegou MC et al (1991) Utilisation des bandes spectrales du vert et du rouge pour une meilleure évaluation des formations végétales actives. In: Congrès AUPELF-UREF. Sherbrooke, Canada
- Darvishzadeh R, Skidmore A, Schlerf M et al (2008) LAI and chlorophyll estimation for a heterogeneous grassland using hyperspectral measurements. *ISPRS J Photogramm Remote Sens* 63:409–426. <https://doi.org/10.1016/J.ISPRSJPRS.2008.01.001>
- de la Rosa JM, Conesa MR, Domingo R, Pérez-Pastor A (2014) A new approach to ascertain the sensitivity to water stress of different plant water indicators in extra-early nectarine trees. *Sci Hortic (amsterdam)* 169:147–153. <https://doi.org/10.1016/j.scienta.2014.02.021>
- de la Rosa JM, Conesa MR, Domingo R et al (2016) Combined effects of deficit irrigation and crop level on early nectarine trees. *Agric Water Manag* 170:120–132. <https://doi.org/10.1016/j.agwat.2016.01.012>
- de Nicola E, Aburizaiza O, Siddique A et al (2015) Climate change and water scarcity: the case of Saudi Arabia. *Ann Glob Heal* 81:342–353
- Di Renzo JA, Casanoves F, Balzarini MG et al. (2019) InfoStat versión 2019
- Gamon JA, Surfus JS (1999) Assessing leaf pigment content and activity with a reflectometer. *New Phytol* 143:105–117. <https://doi.org/10.1046/j.1469-8137.1999.00424.x>
- Georgiou A (2000) Performance of 'nova' mandarin on eleven rootstocks in Cyprus. *Sci Hortic (amsterdam)* 84:115–126. [https://doi.org/10.1016/S0304-4238\(99\)00120-X](https://doi.org/10.1016/S0304-4238(99)00120-X)
- Ginestar C, Castel JR (1996) Responses of young clementine citrus trees to water stress during different phenological periods. *J Hortic Sci Biotechnol* 71:551–559. <https://doi.org/10.1080/14620316.1996.11515435>
- Goldhamer D, Fereres E (2001) Irrigation scheduling protocols using continuously recorded trunk diameter measurements. *Irrig Sci* 20:115–125. <https://doi.org/10.1007/s002710000034>
- Goldhamer D, Fereres E (2004) Irrigation scheduling of almond trees with trunk diameter sensors. *Irrig Sci* 23:11–19. <https://doi.org/10.1007/s00271-003-0088-0>
- Goldhamer D, Soler M, Salinas M et al (2000) Comparison of continuous and discrete plant-based monitoring for detecting tree water deficits and barriers to grower adoption for irrigation management. *Acta Hortic* 537(431):445. <https://doi.org/10.17660/ActaHortic.2000.537.51>
- González-Altozano P, Castel JR (1999) Regulated deficit irrigation in "Clementina de Nules" citrus trees. I. Yield and fruit quality effects. *J Hortic Sci Biotechnol* 74:706–713. <https://doi.org/10.1080/14620316.1999.11511177>
- González-Altozano P, Castel JR (2000) Effects of regulated deficit irrigation on "clementina de nules" citrus trees growth, yield and fruit quality. *Acta Hortic* 537:749–758. <https://doi.org/10.17660/ActaHortic.2000.537.89>
- Gosling SN, Arnell NW (2016) A global assessment of the impact of climate change on water scarcity. *Clim Change* 134:371–385. <https://doi.org/10.1007/s10584-013-0853-x>

- Huang XM, Huang HB, Gao FF (2000) The growth potential generated in citrus fruit under water stress and its relevant mechanisms. *Sci Hortic (amsterdam)* 83:227–240. [https://doi.org/10.1016/S0304-4238\(99\)00083-7](https://doi.org/10.1016/S0304-4238(99)00083-7)
- Hunt ER, Rock BN (1989) Detection of changes in leaf water content using Near- and Middle-Infrared reflectances. *Remote Sens Environ* 30:43–54. [https://doi.org/10.1016/0034-4257\(89\)90046-1](https://doi.org/10.1016/0034-4257(89)90046-1)
- IUSS working group WRB (2015) World reference base for soil resources 2014, update 2015: International soil classification system for naming soils and creating legends for soil maps. Rome
- Jones HG (2004) Irrigation scheduling: advantages and pitfalls of plant-based methods. *J Exp Bot* 55:2427–2436. <https://doi.org/10.1093/JXB/ERH213>
- Kittler J, Illingworth J (1985) On threshold selection using clustering criteria. *IEEE Trans Syst Man Cybern SMC* 15:652–655. <https://doi.org/10.1109/TSMC.1985.6313443>
- Marsal J, Gelly M, Mata M et al (2002) Phenology and drought affects the relationship between daily trunk shrinkage and midday stem water potential of peach trees. *J Hortic Sci Biotechnol* 77:411–417. <https://doi.org/10.1080/14620316.2002.11511514>
- Merzlyak MN, Gitelson AA, Chivkunova OB, Rakitin VY (1999) Non-destructive optical detection of pigment changes during leaf senescence and fruit ripening. *Physiol Plant* 106:135–141. <https://doi.org/10.1034/j.1399-3054.1999.106119.x>
- Ministerio de Agricultura Pesca y Alimentación del Gobierno de España. (2020) Superficies y producciones de cultivos. NIPO 003-19-051-9
- Moriana A, Pérez-López D, Prieto MH et al (2012) Midday stem water potential as a useful tool for estimating irrigation requirements in olive trees. *Agric Water Manag* 112:43–54. <https://doi.org/10.1016/j.agwat.2012.06.003>
- Myers BJ (1988) Water stress integral—a link between short-term stress and long-term growth. *Tree Physiol* 4:315–323. <https://doi.org/10.1093/treephys/4.4.315>
- Naor A (2000) Midday stem water potential as a plant water stress indicator for irrigation scheduling in fruit trees. *Acta Hortic* 537:447–454. <https://doi.org/10.17660/ActaHortic.2000.537.52>
- Naor A, Cohen S (2003) Sensitivity and variability of maximum trunk shrinkage, midday stem water potential, and transpiration rate in response to withholding irrigation from field-grown apple trees. *HortScience* 38:547–551. <https://doi.org/10.21273/HORTSCI.38.4.547>
- Ortuño MF, Alarcón JJ, Nicolás E, Torrecillas A (2005) Sap flow and trunk diameter fluctuations of young lemon trees under water stress and rewating. *Env Exp Bot* 54:155–162. <https://doi.org/10.1016/j.envexpbot.2004.06.009>
- Ortuño MF, García-Orellana Y, Conejero W et al (2006) Stem and leaf water potentials, gas exchange, sap flow, and trunk diameter fluctuations for detecting water stress in lemon trees. *Trees—Struct Funct* 20:1–8. <https://doi.org/10.1007/s00468-005-0004-8>
- Ortuño MF, Brito JJ, García-Orellana Y et al (2009) Maximum daily trunk shrinkage and stem water potential reference equations for irrigation scheduling of lemon trees. *Irrig Sci* 27:121–127. <https://doi.org/10.1007/s00271-008-0126-z>
- Pagán E, Robles JM, Temnani A et al (2022) Effects of water deficit and salinity stress on late mandarin trees. *Sci Total Env* 803:150109. <https://doi.org/10.1016/J.SCITOTENV.2021.150109>
- Panigrahi P, Sharma RK, Hasan M, Parihar SS (2014) Deficit irrigation scheduling and yield prediction of ‘kinnow’ mandarin (*Citrus reticulata* Blanco) in a semiarid region. *Agric Water Manag* 140:48–60. <https://doi.org/10.1016/J.AGWAT.2014.03.018>
- Pérez-Pastor A, Domingo R, Torrecillas A, Ruiz-Sánchez MC (2009) Response of apricot trees to deficit irrigation strategies. *Irrig Sci* 27:231–242. <https://doi.org/10.1007/S00271-008-0136-X>
- Pérez-Pérez JG, Romero P, Navarro JM, Botía P (2008) Response of sweet orange cv “lane late” to deficit irrigation in two rootstocks. I: water relations, leaf gas exchange and vegetative growth. *Irrig Sci* 26:415–425. <https://doi.org/10.1007/s00271-008-0106-3>
- Python Core Team (2015) Python: a dynamic, open source programming language
- Raj R, Suradhaniwar S, Nandan R et al (2020) Drone-based sensing for leaf area index estimation of citrus canopy. In: Jain K, Khoshelham K, Zhu X, Tiwari A (eds) Proceedings of UASG 2019. Springer International Publishing, Cham, pp 79–89
- Romero P, Navarro JM, Pérez-Pérez J et al (2006) Deficit irrigation and rootstock: Their effects on water relations, vegetative development, yield, fruit quality and mineral nutrition of *Clemenules* mandarin. *Tree Physiol* 26:1537–1548. <https://doi.org/10.1093/TREEPHYS/26.12.1537>
- Rouse JWJ, Haas RH, Schell JA et al (1974) Monitoring vegetation systems in the great plains with erts. *NASA Spec Publ* 351:309
- Ru C, Hu X, Wang W et al (2021) Signal intensity of stem diameter variation for the diagnosis of drip irrigation water deficit in grapevine. *Hortic*. <https://doi.org/10.3390/HORTICULTURAE7060154>
- Schneider CA, Rasband WS, Eliceiri KW (2012) NIH Image to ImageJ: 25 years of image analysis. *Nat Methods* 9:671–675
- Shackel KA, Ahmadi H, Biasi W et al (1997) Plant water status as an index of irrigation need in deciduous fruit trees. *HortTechnology* 7:23–29. <https://doi.org/10.21273/HORTTECH.7.1.23>
- SIAM—Sistema de Información Agrario de Murcia (2019) Informe agrometeorológico. In: MU52 “Cabezo plata.” <http://siam.imida.es>. Accessed 29 Jun 2021
- Temnani A, Conesa MR, Ruiz M et al (2020) Irrigation protocols in different water availability scenarios for ‘crimson seedless’ table grapes under mediterranean semi-arid conditions. *Water* 13:22. <https://doi.org/10.3390/w13010022>
- Thenkabail PS, Lyon J, Huete A (2011) Advances in Hyperspectral Remote Sensing of Vegetation and Agricultural Croplands. In: Thenkabail PS, Lyon JG (eds) Hyperspectral Remote Sensing of Vegetation, 1st edn. CRC Press, Boca Raton, USA, pp 39–74
- Yu K, Gnyp ML, Gao L et al (2015) Estimate leaf chlorophyll of rice using reflectance indices and partial least squares. *Photogramm Fernerkundung, Geoinf* 2015:45–54. <https://doi.org/10.1127/PFG/2015/0253>
- Zarco-Tejada PJ, Ustin SL (2001) Modeling canopy water content for carbon estimates from MODIS data at land EOS validation sites. *Int Geosci Remote Sens Symp* 1:342–344. <https://doi.org/10.1109/IGARSS.2001.976152>
- Zhihui C, Liangcheng Z, Guanglin WU, Shonglong Z (1990) Photosynthetic acclimation to water stress in citrus. *Proc Int Citrus Symp* 5–8:413–418

**Publisher's Note** Springer Nature remains neutral with regard to jurisdictional claims in published maps and institutional affiliations.